fore not negligible, and the values of A used here are somewhat in error.

Instead of using the static lattice bulk moduli and lattice constants to evaluate the Born-Mayer potential parameters, as would be correct, the room temperature values of K and R_0 were used. It is estimated that the static lattice compressibility is about 10% lower than the observed room temperature compressibility and that the lattice constant of the static lattice is a few percent lower than the observed room temperature value.[1] This correction will be neglected here, such a refinement being unwarranted by other approximations in the theory.

SUMMARY

The results of this study may be briefly summarized as follows: The mechanisms of polarization described in Sec. IV must be responsible for at least part of the deviations of e^*/e from unity. These mechanisms also give a qualitative explanation of the deviations of the so-called crystal polarizabilities from the free-ion polarizabilities. The explanation of the deviations of K^*/K from unity is to be sought in a more sophisticated theory of the elastic constants than that used here. The model of the short-range repulsive interaction in terms of the exchange charge introduces many-body forces into a Born-Mayer type model of the crystal.

PHYSICAL REVIEW VOLUME 112, NUMBER 1 OCTOBER 1, 1958

Study of Reactor-Irradiated α-Al_2O_3†

J. J. ANTAL, *Ordnance Materials Research Office, Watertown, Massachusetts, and Brookhaven National Laboratory, Upton, New York*

AND

A. N. GOLAND, *Brookhaven National Laboratory, Upton, New York*

(Received May 28, 1958)

Studies are presented here on reactor-irradiated alpha aluminum-oxide single crystals. These are a continuation of the use of long-wavelength neutron transmission for determining the concentration and types of defects produced in solids by high-energy particle irradiation. The material exhibited crystallographic stability to fast-neutron irradiation at temperatures <40°C, and the results indicate a total number of defects approximately 40 times less than that predicted by current theories. Correlation with macroscopic density changes is good. Examination of the wavelength dependence of the neutron scattering indicated that the damage may be partly Al-O vacancy pairs at room temperature. Annealing of the material produced no decrease in the concentration of defects from room temperature to 400°C, a steady decrease from 400°C to 1250°C, and nonuniform changes in neutron scattering and visually observable optical coloring beyond 1250°C. Annealing at a temperature of 1800°C did not remove the coloring, although the density returned to its pre-irradiation value.

I. INTRODUCTION

SOME earlier experiments concerning the use of neutron spectroscopy for the determination of point defects in irradiated graphite[1] gave promising results. The experiments to be described here are primarily a continuation of this work. The technique is simply a measurement of the scattering of long-wavelength neutrons by crystallographic defects in a solid. It is unique in its ability to give a direct measure of the number of defects in a material without an undue number of assumptions. As a result of the low neutron intensity which is presently available for wavelengths greater than 4 or 5 angstroms, only concentrations of defects of 0.1% or greater are readily detectable. For the same reason the experiment must be restricted to materials which have a low capture cross section and a high bound-atom coherent scattering cross section, and which will retain large numbers of defects at temperatures where irradiation and examination are possible. It was expected that the strong, mostly ionic bonding in α-aluminum oxide (corundum) would lead to retention of defects at the temperatures available for this irradiation (always less than 40°C). Also, the low capture cross sections of the constituent nuclei made this a favorable material. As explained in the next section, complicating features of this material are its complex crystal structure and its diatomic nature.

† Work performed under the auspices of the U. S. Atomic Energy Commission.

[1] Antal, Weiss, and Dienes, Phys. Rev. 99, 1081 (1955).

II. BASIC CONSIDERATIONS

A. Neutron Transmission

(*1*) *Monatomic material.*—If one considers the scattering of slow neutrons by isolated, randomly arranged point defects in a crystal lattice, for wavelengths sufficiently long that Bragg scattering is not possible, the atomic fraction of such defects is simply[1] given by

$$f=\sigma_d/\sigma_s.$$

Here, σ_d is the cross section per atom for scattering by

the defects alone, and σ_s is the scattering cross section per defect, equal in this instance to the bound-atom coherent scattering cross section, which is determined from other experiments and has been tabulated.[2] The cross section σ_d is determined by measuring the transmission of the material containing the defect scatterers. It should be mentioned at this time that more information on the nature of the defects would be forthcoming if the differential cross section, i.e., the angular distribution of the scattered intensity, could be measured. Because of the relatively high radiation backgrounds near a nuclear reactor, it is only practicable to measure the total amount of scattered intensity and even so the quantities are measured with difficulty.

In order to increase the sensitivity and accuracy of the experiment, the intensity transmitted by an irradiated specimen relative to that transmitted by an unirradiated but otherwise identical specimen is measured. This procedure eliminates the need for employing inaccurately known values for other neutron interaction processes which, although kept purposely small, occur in addition to the defect scattering. Lattice inelastic scattering, spin and isotope incoherent scattering, and capture are such sources of attenuation. In the case of monatomic materials, the concentration of defect scatterers is given directly by

$$f=[-\ln(I_i/I_u)][NX\sigma_s]^{-1}, \tag{1}$$

where, I_i and I_u are the intensities transmitted through the irradiated and unirradiated specimens, respectively, N is the number of atoms per unit volume in the material, and X is the length of the specimen traversed by the neutron beam.

(2) *Diatomic material.*—The expression in Eq. (1) is to be contrasted with the following development for the case of a diatomic substance. The relations given below have been generalized to include the possibility that there may be clusters of defects such as pairs present in addition to point scatterers. The intensity transmitted through such a material before irradiation is given by

$$I_u=I_0\exp[-X_u(N_u{}^a\sigma_c{}^a+N_u{}^b\sigma_c{}^b+N_u{}^m\sigma_u{}^m)], \tag{2}$$

where the superscripts a and b designate the two kinds of atoms present, N_u is the number of atoms per unit volume, σ_c is the capture cross section, and σ_u is any additional scattering cross section (lattice inelastic, etc.) attributable only to the whole molecule, m. Under the assumption that clusters in the form of pairs are created the expression for the transmitted intensity after the specimen has been irradiated is

$$I_i=I_0\exp[-X_i(N_i{}^a\sigma_c{}^a+N_i{}^b\sigma_c{}^b+N_i{}^m\sigma_i{}^m+N_d{}^a\sigma_s{}^a+N_d{}^b\sigma_s{}^b+\textstyle\sum_j N_p{}^j\sigma_p{}^j)]. \tag{3}$$

Here, the subscript i pertains to the irradiated specimen, and N_d is the number of isolated point defects per unit volume (both interstitials and vacancies). The subscript p refers to those point defects which are associated with one another as pairs and $N_p{}^j$ is the number of isolated pairs of type j per unit volume. The sum over j takes into account the fact that there may be different types of pairs such as vacancy-vacancy (V-V) pairs, interstitial-interstitial (I-I) pairs and interstitial-vacancy (I-V) pairs. Moreover, the individual defects comprising a pair may be different kinds of atoms. Each of these various pairs has a scattering cross section $\sigma_p{}^j$ which is different from the sum of the two appropriate coherent scattering cross sections. This difference will be discussed in more detail shortly. For a fixed experimental geometry, X_i will include any physical expansion of the specimen caused by the production of defects. We define the fraction of isolated point defects of kind a as

$$f^a=N_d{}^a/(q^a+q^b)N^m, \tag{4}$$

and the fraction of isolated pairs of type j as

$$f_p{}^j=N_p{}^j/(q^a+q^b)N^m, \tag{4a}$$

where q^a is the number of atoms of kind a per molecule and similarly for q^b. Division of (2) by (3) with the substitution of (4) gives the combined result

$$f^a+\left(\frac{\sigma_s{}^b}{\sigma_s{}^a}\right)f^b+\sum_j f_p{}^j\left(\frac{\sigma_p{}^j}{\sigma_s{}^a}\right)=\frac{\ln(I_u/I_i)+(q^a\sigma_c{}^a+q^b\sigma_c{}^b)(X_uN_u{}^m-X_iN_i{}^m)+(X_uN_u{}^m\sigma_u{}^m-X_iN_i{}^m\sigma_i{}^m)}{N_i{}^mX_i(q^a+q^b)\sigma_s{}^a}. \tag{5}$$

The coherent scattering cross section is used for σ_s just as before. The first term on the right-hand side of (5) is determined by making a relative transmission measurement of an irradiated and an unirradiated specimen. The next two terms express any differences in length or in other scattering cross sections as a result of irradiation. To the accuracy expected in the present work, it can be assumed that differences in other scattering cross sections are unimportant.[3] The first two terms on the left are self explanatory; the third term will now be explained in more detail.

(3) *Clusters of defects.*—There is experimental evidence that clusters of defects are produced in neutron-irradiated material. These clusters may be a direct result of the nature of the damaging process.[4] In addition, we may suppose that migration produces randomly distributed groups of defects such as pairs or larger clusters. Any such association of defects brings interference effects into the scattering. Consider the simplest association, a pair of point defects, 1 and 2. We may describe pair scattering as molecular scattering to a

[2] *Neutron Cross Sections,* compiled by D. J. Hughes and J. A. Harvey, Brookhaven National Laboratory Report BNL-325 (Superintendent of Documents, U. S. Government Printing Office, Washington, D. C., 1955), pp. 3 ff.

[3] G. J. Dienes and G. H. Vineyard, *Radiation Effects in Solids* (Interscience Publishers, Inc., New York, 1957), p. 72.

[4] Truell, Teutonico, and Levy, Phys. Rev. **105**, 1723 (1957).

sufficient degree of approximation by adaptation of the treatment originally developed by Debye.[5] The scattered wave is given by

$$\psi=\pm\alpha_1\exp(-i\mathbf{s}\cdot\mathbf{r}_1)\pm\alpha_2\exp(-i\mathbf{s}\cdot\mathbf{r}_2).$$

Here, r_i is the vector distance from an arbitrary origin to the defect in question, α_1 and α_2 are the respective scattering amplitudes of the atoms, 1 and 2, and $|s|=4\pi\sin\theta/\lambda$ (θ is half the scattering angle, and λ is the neutron wavelength). If we define the separation between defects as $\mathbf{R}=\mathbf{r}_1-\mathbf{r}_2$, then the differential cross section is

$$\sigma(\theta)=|\psi|^2$$
$$=\alpha_1^2+\alpha_2^2\pm\alpha_1\alpha_2[\exp(-i\mathbf{s}\cdot\mathbf{R})+\exp(+i\mathbf{s}\cdot\mathbf{R})]$$
$$=\alpha_1^2+\alpha_2^2\pm2\alpha_1\alpha_2\cos(\mathbf{s}\cdot\mathbf{R}).$$

Averaging over all orientations of the pair, we obtain

$$\sigma_{\text{pair}}(\theta)=\alpha_1^2+\alpha_2^2\pm2\alpha_1\alpha_2\frac{\sin(4\pi R\sin\theta/\lambda)}{4\pi R\sin\theta/\lambda}. \quad (6)$$

Finally, the total cross section is obtained from (6) as

$$\sigma_{\text{pair}}=(\sigma_s)_1+(\sigma_s)_2\pm8\pi\alpha_1\alpha_2\frac{\sin^2(2\pi R/\lambda)}{(2\pi R/\lambda)^2}. \quad (7)$$

It is this expression which is to be substituted for $\sigma_p{}^i$ in (5). Pairs of similar types of defects (V-V or I-I) require the use of the positive sign with the last term in (7); dissimilar types (I-V), the negative sign. The appropriate cross sections and scattering amplitudes to be used are determined by the kinds of atoms comprising the pair.

At this point a discussion of the significance of (7) in the interpretation of the experimental data is instructive. The first point worth noting is that, in general, the cross section determined in a transmission experiment will consist of contributions from single and clustered defects. The clusters may be of various sorts, and in general, it will be impossible to separate or determine uniquely the types of clusters which are actually present. The way to proceed in the analysis of the data is to plot the right-hand side of (5) as a function of wavelength and initially to ignore the contribution due to pairs or larger clusters on the left-hand side of (5) in determining the fraction of defects. This is equivalent to ignoring the interference term in the scattering cross section of the pairs. Examination of (7) reveals that such action will lead to an overestimate of the number of defects if the pairs have like constituents (I-I or V-V) and to an underestimate if they have unlike constituents (I-V). The pair cross section, however, does manifest itself in the data because it is the only term on the left-hand side of (5) which contains a dependence upon wavelength. Therefore, the appearance of a wavelength dependence in the data will indicate the presence of clusters, perhaps pairs.

One other consequence of the presence of clusters must be mentioned. It is well known from small-angle scattering theory that as the size of a cluster increases, it scatters progressively more in the forward direction. There is thus some limitation to the size of a cluster which can be detected by this transmission experiment; if the cluster is too large the scattered intensity enters the counter as a constituent of the direct beam. The size of the largest cluster which will be detected is determined by the geometry of the experiment and may be estimated roughly with small-angle scattering theory.[6] For the sensitivity of this particular experiment clusters of average radius of gyration greater than approximately 500 A will not be detected; if large clusters are present the number of defects is underestimated. It will be helpful to bear these facts in mind when reading the discussion which follows on the application of this technique to irradiated Al_2O_3.

B. Displacements Produced by Fast Neutrons

The theoretical value for the number of atoms displaced may be calculated from the work of Kinchin and Pease.[7] Their expression for the number of atoms displaced on the average for each neutron collision is, for these relatively light elements O and Al where all excess energy is lost to ionization,

$$N_D=(2-L_c/E_{\max})L_c/4E_d. \quad (8)$$

Here E_d is the energy required for displacement of an atom from its lattice site, taken here to be uniformly 25 ev, and $E_{\max}$ is the maximum energy transferred to an atom by an impinging neutron, a quantity which depends upon the energy of the bombarding neutron and the masses of the neutron and the atom. L_c is the threshold energy for ionization and is given approximately by $(M/m)I_t/8$, where M is the mass of the moving atom, m is the electron mass, and I_t is the energy corresponding to the edge of the first main optical absorption band. The number of fast-neutron collisions per unit volume is given by

$$N_n=N\sigma_n\Phi, \quad (9)$$

where σ_n is the average fast-neutron cross section per atom in the material and Φ is the total neutron flux (nvt). The theoretical fraction of defects is given by twice the product of Eqs. (8) and (9) divided by the total number of atoms per unit volume N. Thus,

$$f=2\sigma_n\Phi N_D. \quad (9a)$$

[5] See general discussions in L. O. Brockway, Revs. Modern Phys. 8, 231 (1936); N. S. Gingrich, Revs. Modern Phys. 15, 90 (1943); and M. H. Pirenne, *The Diffraction of X-Rays and Electrons by Free Molecules* (Cambridge University Press, New York, 1946), Chap. VI, pp. 56ff.

[6] R. J. Weiss, Phys. Rev. 83, 379 (1951).

[7] G. H. Kinchin and R. S. Pease, in *Reports on Progress in Physics* (The Physical Society, London, 1955), Vol. XVIII, p. 1.

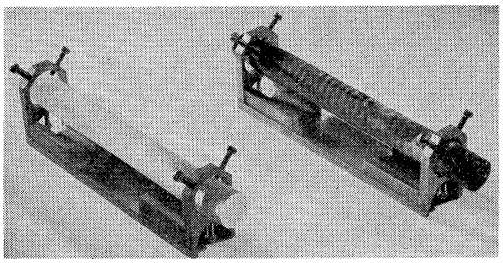

FIG. 1. Photograph of synthetic sapphire crystals used in these studies. The crystal at the left is unirradiated and that at the right has been irradiated to a total fast-neutron flux of $1.2\times10^{19}nvt$. The sample orientation is changed with the screws shown and the orientation is thereafter retained by the tray which accommodates the holders and interchanges their position in the beam. The crystals are approximately $\frac{5}{8}$ inch in diameter and 5 inches in length.

III. EXPERIMENTAL DETAILS

A. Specimens

The specimens employed were two single crystals of Al_2O_3 obtained from Linde as synthetic sapphire. They were approximately 5 inches long and $\frac{5}{8}$ inch in diameter. A photograph of the mounted specimens is Fig. 1.

B. Irradiations

One of the crystals just described was irradiated to a total fast-neutron flux of $1.19\times10^{19}nvt$ in an air-cooled hole of the Brookhaven reactor. It was irradiated in three stages and the effects of the irradiation were investigated after each stage. The temperature of irradiation was always less than 40°C.

C. Transmission Measurements

The source of slow neutrons for the scattering experiment was the Brookhaven graphite-moderated reactor. A primary filter of coarse-grained bismuth is permanently positioned in the beam to reduce the gamma flux density and to attenuate a portion of the high-energy end of the thermal-neutron spectrum. The resultant neutron beam is primarily made up of neutrons of wavelengths greater than 3 A. These neutrons are collimated and passed through a secondary filter to remove the remaining short-wavelength neutrons which are unwanted and might otherwise appear as second-order scattering from the monochromator. A crystal spectrometer is used to analyze the neutron beam as is indicated schematically in Fig. 2.[8] The sample positions are exchanged in the beam in order to obtain a transmission reading, and the crystal monochromator is rotated a small amount in order to eliminate Bragg reflection for a background reading. The spectrometer is programmed to make all measurements automatically in order to utilize all available counting time. The various transmission and background readings are interleaved so as to eliminate any errors due to long-term variations in neutron-beam intensities.

The primary difficulty in the experiment is the low neutron intensity. If we wish to examine aluminum oxide in a wavelength region where Bragg scattering is absent, it is necessary with a powder sample to go to a wavelength $\lambda>2d_{\max}$, where $d_{\max}$ is the largest lattice spacing in the crystal. In Al_2O_3 this wavelength is 6.958 A. The intensities available beyond this wavelength are

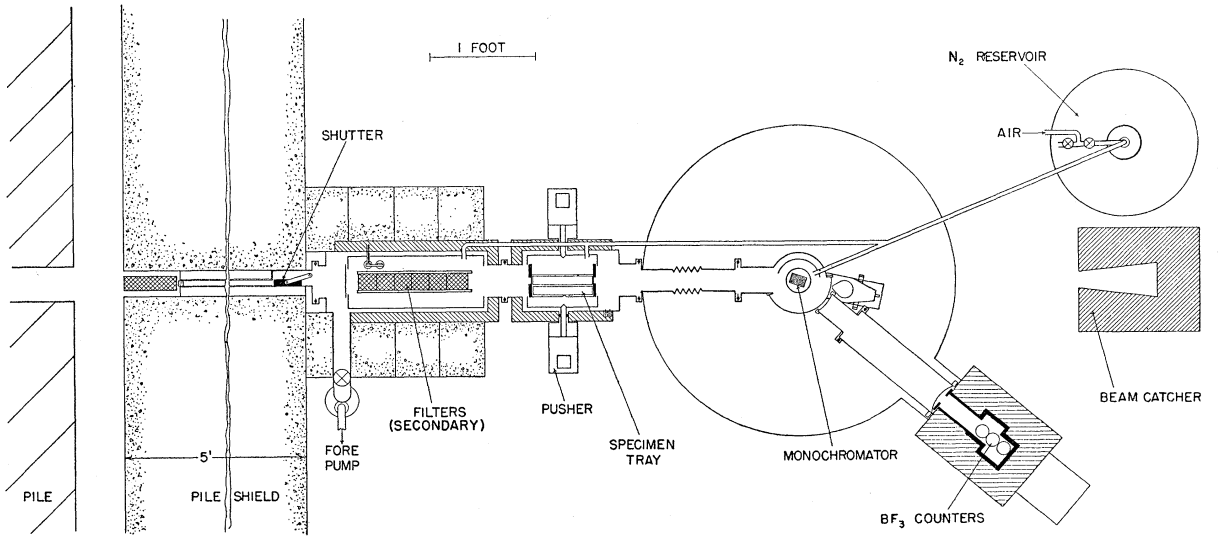

FIG. 2. Horizontal cross section of cold-neutron spectrometer. Neutrons from the reactor at the left pass through the primary and secondary filters, through the specimen, and are analyzed by the crystal monochromator. When beryllium is used as a secondary filter it is cooled with liquid nitrogen to reduce lattice inelastic scattering. The specimens were not cooled, nor was the vacuum beam path to the monochromator and counters employed in the studies described in the text.

[8] A detailed description of the spectrometer is found in J. J. Antal, Materials Research Laboratory Report No. 31, Ordnance Materials Research Office, August, 1957 (unpublished).

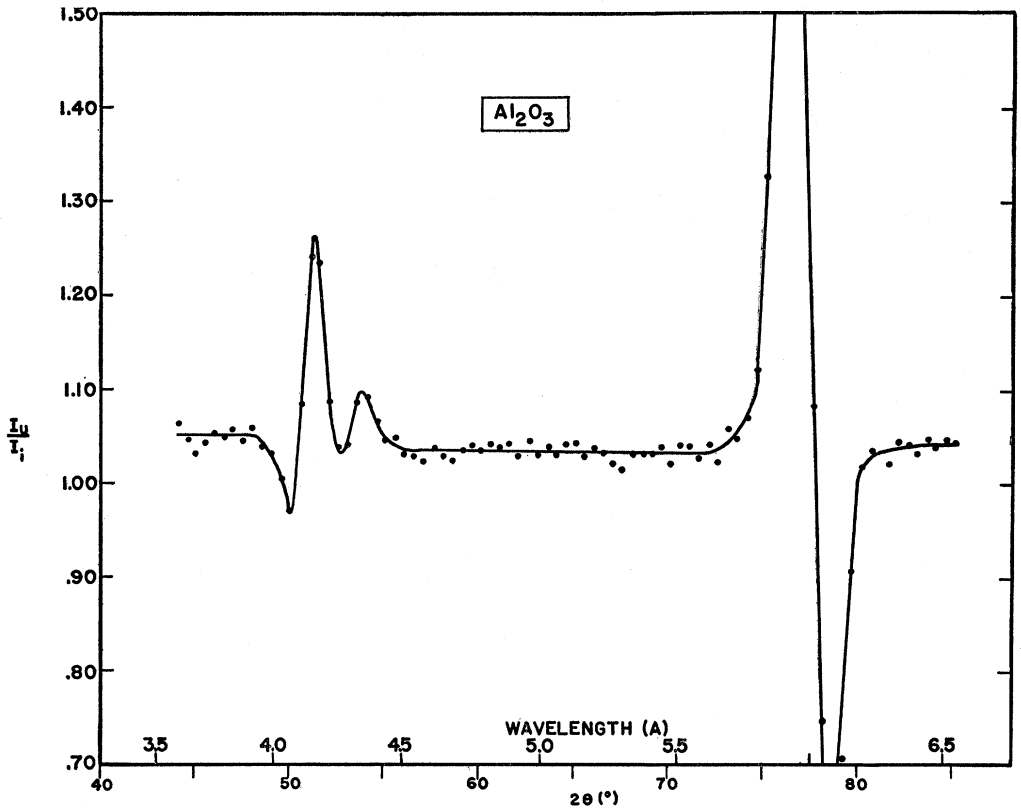

FIG. 3. Relative transmission of unirradiated and irradiated aluminum oxide specimens in the region of the Bragg cutoff. The period of irradiation was 240 days. The peaks are the result of Bragg scattering which is totally absent beyond 6.5 A. The specimens are not oriented identically and therefore peaks appear both above and below the average line. The accuracy of the points presented here is much less than that employed in a determination of the defect concentration.

extremely low. It is possible to employ shorter wavelengths by using single-crystal samples, for which the Bragg scattering is confined to well-defined regions in space and can be eliminated by proper orientation of the crystal with respect to the neutron beam. Actually, it was not possible to obtain crystals of large enough diameter to allow this arrangement, but beyond 4.5 A only one crystalline reflection was found to be present in each specimen, and since the material was quite perfect this peak was narrow.

If the crystal orientations of two specimens are not identical, then a relative transmission measurement should show both a positive and a negative peak in the vicinity of each wavelength for which the Bragg scattering conditions are fulfilled. This arises from the fact that both crystals will not be scattering waves of equal intensity at exactly the same wavelength. Such a measurement for the two Al_2O_3 single crystals used in the present work is shown in Fig. 3. Only the last cutoff is shown and the accuracy of the points in the figure is much less than that employed in a determination of the defect concentration. Since the irradiated specimen had to be removed and replaced in the holder to obtain the various levels of irradiation and annealing, a careful rerun of these peak positions was made each time as a check on the alignment of the crystal positions in the spectrometer.

Figure 4 shows the experimental data obtained with the crystal spectrometer. After the first irradiation, so few scatterers were present that the scattering was not detectable. A truly detectable difference in transmission was noted after about 3.5 times the first dose (second curve). Because of the length of time necessary to take the data, points were obtained approximately 0.5 A apart, and the resolution of these two curves is not

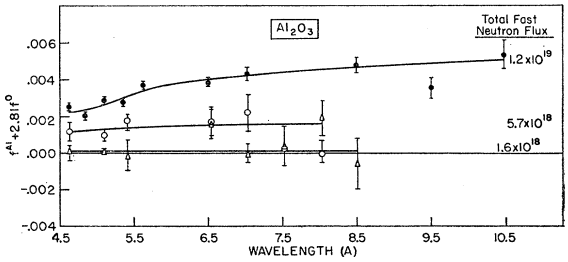

FIG. 4. The quantity $f^{Al}+2.81f^O$ determined by neutron scattering as a function of wavelength. Multiplying the value of the ordinate by 0.479, one obtains f, the concentration of defect scatterers. It is assumed that for each displaced atom there exists a vacancy, and that an aluminum or oxygen atom is displaced with equal probability.

great. It was clear at this point that much improvement in the sensitivity of the apparatus would be necessary before an accurate determination on this material could be made. Accordingly, the spectrometer was revised[8] and then employed in the study of the transmission after the maximum dose (top curve of Fig. 4). Note that the statistical error on this curve is smaller, and is more uniform over the wavelength range examined than for the previous irradiations. Note also that a wavelength dependence of the scattering is present.

D. Density Measurements

It became clear after the first irradiation of the Al_2O_3 that very little damage was being retained by the material after bombardment at room temperatures. No reasonable explanation for this could be found, and it was decided that it would be necessary to obtain some correlation with another physical property. An attempt was made to measure the optical density of thin samples irradiated along with the large neutron-transmission specimen, but all became too dense after the first period of irradiation. Hydrostatic density measurements were tried and found to be the most easily obtainable measurements of sufficient accuracy. The large mass of the samples (approximately 115 g) allowed accurate measurements with a large analytical balance accurate to ± 0.0002 g. The method of hydrostatic weighing was employed using standard techniques.[9,10] The same batch of distilled water was used as the buoyant liquid for each determination, and the standard, unirradiated specimen was weighed immediately after the irradiated specimen. The specimens were hung from the balance arm by a 0.001-inch diameter stainless steel wire with a single loop around the specimen; the total weight of wire was approximately 0.009 g. Air bubbles were removed from around the sample by boiling under vacuum, and corrections were made for the weight of the support wire and the effect of air buoyancy, humidity, and temperature. Since changes in density of the order 0.1% were found, the above precautions proved quite adequate to obtain the necessary accuracy.

E. Annealing Studies

After the determination presented in Fig. 4, the specimen was annealed for one hour at a series of temperatures up to 1800°C. The temperature of the specimen was increased at approximately 3°C per minute to the desired value, maintained at that value for one hour, and then decreased slowly, generally at 3°C per minute until it reached 50% of its maximum value. At this point the furnace was shut off and kept closed. The annealing was carried out in air up to 1000°C and in high vacuum at all higher temperatures. After each annealing process a determination of the neutron transmission of the specimen relative to the standard was made, and the natural logarithm of this number, which is proportional to the fraction of defects, is plotted in Fig. 5. The neutrons used in these determinations were from a filtered beam of high intensity. The neutron counter is set to intercept the direct beam at θ equal to 0°, and a secondary filter is inserted in the beam. The filter is made up of 4 inches of beryllium and 10 inches of graphite and transmits a beam of neutrons whose distribution rises sharply from zero at 6.5 A to a peak intensity near 7.0 A and falls off with increasing wavelength somewhat as λ^{-3}. Thus a fairly sharply peaked intensity distribution is obtained having a large integrated intensity. The effective wavelength of this distribution was obtained as 7.89 A by measuring the transmission of polycrystalline aluminum with this spectrum and comparing the cross section measured with the published cross section *vs.* λ data.[2] The cross section of aluminum is closely proportional to $1/\lambda$ in this wavelength region. The effective wavelength so determined was verified when the value of the transmission for the fully irradiated specimen was inserted in Eq. (5) and the value of f fell correctly upon the curve of Fig. 4.

IV. DISCUSSION

A. Neutron Transmission and Density Changes

If, as suggested earlier, the presence of clusters is initially ignored, then reference to Eq. (5) shows that the experimental data furnish the quantity $f^{Al}+(\sigma_s{}^O/\sigma_s{}^{Al})f^O$. Since $\sigma_s{}^O=4.24$ barns and $\sigma_s{}^{Al}=1.51$ barns, this quantity becomes $f^{Al}+2.81f^O$ and is equal to the ordinate in Fig. 4. If one assumes an equal probability for displacement of Al and O atoms, it is easy to show that the total fraction of defects is

$$f=f^{Al}+f^O=(5/3)f^O, \tag{10}$$

and that

$$f^{Al}=(2/3)f^O. \tag{11}$$

From (10) and (11) it follows directly that

$$f=0.479(f^{Al}+2.81f^O). \tag{12}$$

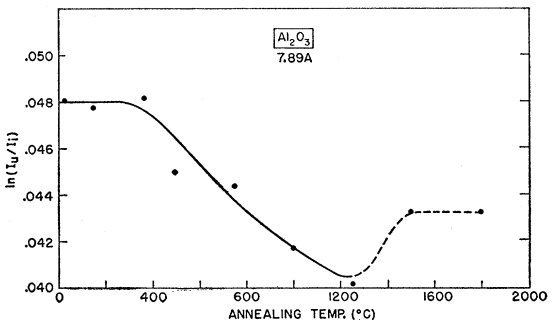

FIG. 5. The measured change in the scattering by defects in the irradiated specimen as annealing proceeded. The dashed portion of the curve is not representative of the removal of defects by annealing, but rather of a change in their character and is not readily analyzed from this presentation.

[9] N. Bauer, in *Physical Methods of Organic Chemistry*, edited by A. Weissberger (Interscience Publishers, Inc., New York, 1949), Chap. VI.

[10] A. Smakula and V. Sils, Phys. Rev. **99**, 1744 (1955).

By means of Eqs. (8) and (9) it is possible to make a theoretical estimate of the number of defects created by neutron irradiation of Al_2O_3, according to the theory of Kinchin and Pease. If the average neutron energy is 1 Mev, and the atomic weight of the bombarded atoms is taken to be the weighted average mass of an aluminum and an oxygen atom, then E_{max} is of the order of 0.18 Mev. The energy corresponding to the edge of the first main optical absorption band in Al_2O_3 is 9 ev. This leads to an approximate value for L_c of 4.2×10^4 ev. Substituting these numbers into Eq. (9a), we can arrive at the values of f shown in Table I for the three integrated neutron fluxes to which the Al_2O_3 was subjected. Experimental values of f taken from Fig. 4 at 5 A are included for comparison. Thus, the theoretical values resulting from the theory of Kinchin and Pease are at least 40 times greater than the experimental values.

A careful survey was made for any experimental problems which might have given rise to the small value of f, but none could be found. One suspected source of difficulty was the possibility of annealing caused by abnormal heating of the specimen during irradiation. A separate check was made on the temperatures involved in this procedure with a dummy sample inserted in the irradiation facility in exactly the same manner, with temperatures monitored on the sample container and at the center of the specimen during irradiation. Cooling of the specimen was found to be sufficient to keep the interior of the specimen within 20°C of the cooling-air temperature, even during rapid temperature excursions. The temperature of the cooling air was always below 40°C.

Since little else is known of the displacement of atoms in corundum, it is thought that annealing at the temperature of irradiation is responsible for the small number of defects determined. This low value for defect concentration is also in agreement with reported optical transmission data for lower doses[11] if one assumes that the number of defects is proportional to the number of color centers produced upon irradiation.

As mentioned previously, a study of the wavelength dependence of the neutron transmission will give further information about the character of the scatterers involved. The variation with wavelength exhibited by the data is not large, but the scattering from simple multiple defects is not expected to be large either. Were there no dependence upon wavelength, the ordinate of the experimental data in Fig. 4 would give the fraction of defects f correctly when inserted in parentheses in Eq. (12), and it could be assumed that the defects were simply vacancies and/or interstitials. The appearance of a wavelength dependence necessitates the replacement of σ_s and makes the factor 2.81 in the ordinate incorrect. It is possible to calculate the expected cross section for groups of point defects to a fair degree of accuracy, however, from Eq. (7). A plot of the cross sections for expected pairs of defects in Al_2O_3 is given in Fig. 6. For clarity, only the wavelength-dependent last term of Eq. (7) designated as $F(\lambda)$ is plotted, the absolute cross sections being unimportant because of the indeterminacy of f. The curves were calculated for several expected positions of vacancy sites in the Al_2O_3 structure and for aluminum interstitial sites which are probable. The structure of corundum is best visualized as an array of almost close-packed oxygen atoms with aluminum atoms in some of the octahedral holes.[12] The aluminum atoms are approximately $\frac{1}{2}$ the radius of the oxygen atoms, and reside comfortably in the octahedral holes, displaced toward one apex. It seems proper to assume that upon annealing some of the displaced aluminum atoms will move into the octahedral holes normally vacant in the corundum structure. It is these interstitial positions for which the interstitial-vacancy (I-V) calculations were made. The positions and separations of interstitial oxygen atoms are not easily determined and were not included in the calculations. The curves of Fig. 6 may be compared directly to those of Fig. 4 in regard to their shape. When this is done, it is seen that none of the curves for the simple pairs is precisely similar to the experimentally determined curves. Perhaps if any of the simple pair models presented is to be chosen as

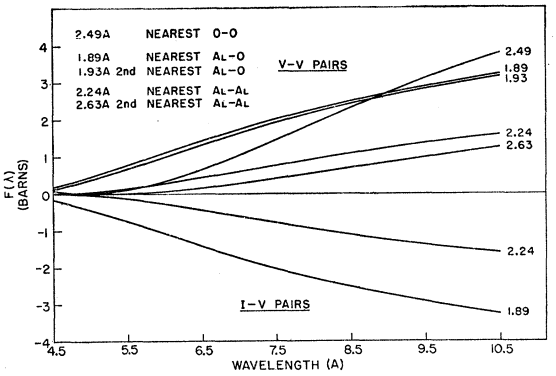

FIG. 6. Theoretical values for the wavelength-dependent portion of the cross section for pairs of defects. The I-V curves shown are for interstitial aluminum and vacancy oxygen sites. Although values for interstitial-interstitial (I-I) pairs are not shown, they would have positive values of $F(\lambda)$ similar to (V-V) pairs.

TABLE I. Comparison of the fraction of defects in Al_2O_3 as calculated according to the theory of Kinchin and Pease with the experimentally determined fraction for the three integrated neutron fluxes employed.

$\Phi(nvt)$	$f(K-P)$	f(exp)
1.6×10^{18}	0.74%	~0.01%
5.7×10^{18}	2.6%	~0.06%
9.2×10^{19}	5.5%	~0.12%

[11] P. W. Levy, as quoted in reference 3, pp. 81–82; P. W. Levy, Bull. Am. Phys. Soc. Ser. II, 3, 116 (1958).

[12] R. W. G. Wycoff, *Crystal Structures* (Interscience Publishers, Inc., New York, 1951), Vol. I.

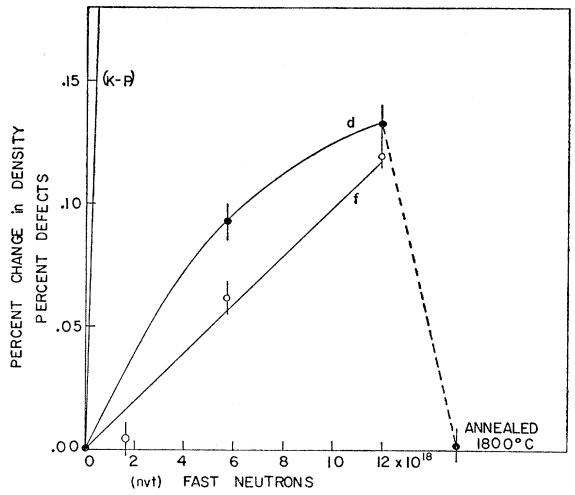

FIG. 7. The experimentally determined fraction of defects f in percent and the absolute value of the percent change in the hydrostatic density d as a function of bombarding flux. The density decreased with increasing neutron dose. The values of f have been determined from the curves of Fig. 4 at 5 A. Also shown is the fraction of defects predicted by the theory of Kinchin and Pease (K-P). The value of the density after the fully irradiated crystal was annealed at 1800°C is seen to be closely that of the original, unirradiated state of the crystal.

represented in the experimental data, nearest neighbor aluminum-vacancy-oxygen-vacancy pairs are the most probable as determined from the slope of the curves near 5 A. One must be careful to remember that the models presented do not give unique curvatures to $F(\lambda)$; it is possible to devise other configurations of defects which will give the same curvature. Note that if both like pairs (I-I or V-V) and unlike pairs (I-V) are present in equal numbers and have equal scattering cross sections and interatomic separations, they have a cancelling effect since $F(\lambda)$ has a different sign in each case. If this were the case the correct value of f would be given directly by the experiment. However, it is thought that such a situation would be fortuitous and it is not considered as a likely possibility.

A general picture of the history of the specimen can be seen in Fig. 7, where f and the absolute value of the percent change in hydrostatic density d are presented as a function of neutron bombarding flux. The density was found to decrease with increasing exposure to reactor radiation. The values of f have been obtained at 5 A from Fig. 4 since Fig. 6 shows that the wavelength dependence of the pair scattering cross section is negligible in this region. Note that the density change follows the change in f, and that the theoretically calculated fraction of defects is much larger per unit fast-neutron flux than the measured fraction. An interesting feature of these curves is that the fractional change in density is always greater than the fraction of defects present in the crystal. This fact can be explained by taking into account the ionic nature of the binding in Al_2O_3. A likely consequence of such binding is that the lattice relaxation is outward around a vacancy as well as around an interstitial. This would lead to the effect shown in Fig. 7 even if the concentrations of vacancies and interstitials were unequal. However, in the absence of a refined theoretical treatment of such an effect, it is felt that further comments should be reserved for the future.

B. Annealing

No change in the neutron scattering was noted up to 400°C, after which the scattering decreased up to a temperature of 1250°C. A change in the character of the annealing (to be described later) was noted at the 1250°C temperature and at the two points beyond, and a corresponding irregularity in the neutron scattering was noted. Because the wavelength dependence of the scattering was changing markedly, it is felt that the points beyond 1250°C are not representative of the number of defect scatterers, but rather of their character. This was further verified when a wavelength dependence run similar to those of Fig. 4 was made after the 1800°C anneal. An extremely irregular curve was found which would be very difficult to analyze and therefore is not reproduced here.

The annealing of the specimen proceeded as a uniform bleaching of the very dark brown color of the fully-irradiated specimen to a light amber at 1000°C. At 1250°C the color was an even lighter amber, but a darker core was visible along the long axis of the crystal. At 1500°C the over-all color was an extremely pale blue with a dark blue core, and at 1800°C the over-all color was clear (representative of the unirradiated state of the crystal), but the dark core remained, now returning to a dark brown. Clearly, large changes in the character of the crystal were taking place in the annealing range above 1250°C and these correlated with the neutron results. As Fig. 7 indicates, the density of the specimen after the 1800°C anneal was practically equal to its original, pre-irradiation value.

Further study is being made on the coloration of the crystal, but it is felt that the following is true. The light blue coloration of the specimen after annealing at 1500°C was a Tyndall effect produced by particles or bubbles of colloidal dimension. Although a similar core type of coloration was noted by Cutler, Bates, and Gibbs[13] and in fact could be produced by them at will by prolonged heating (>12 hr) of the crystals at high temperatures in oxygen atmospheres, the fact that our crystal was annealed in a vacuum for temperatures 1250°C and above for only one hour would appear to preclude any similarity in the production. The production of the effect may depend upon the purity of the crystal, and upon the thermal stresses set up in the crystal during heat treatment.[14] Experiments have shown, for instance, that no such coloring can be pro-

[13] Cutler, Bates, and Gibbs, Bull. Am. Phys. Soc. Ser. II, 2, 300 (1957).

[14] The authors are indebted to P. W. Levy for a valuable discussion concerning the heat treatment of aluminum oxide crystals.

duced in ultrapure Al_2O_3. On the other hand, when Al_2O_3 containing trace impurities is subjected to the proper heat treatment the impurities precipitate along certain crystallographic axes. This is the manner in which synthetic star sapphires are manufactured, and a great deal of effort has been put into developing the correct conditions of heating. Evidently in the experiments described in this paper the same phenomenon resulted without regard for the type of heat treatment employed. It may be that the irradiation produced enough residual stress in the crystal to make the stress resulting from the heat treatment much less important than it is in an unirradiated crystal. With regard to the impurities, it is not known at present whether they precipitate on dislocations or on clusters of defects or whether some other mechanism is responsible for their agglomeration. It is not difficult to imagine that various defects are introduced during crystal growth, and that these migrate to the center of the crystal during the heating process forming complex centers upon which the impurities precipitate.

V. CONCLUSIONS

In conclusion, this work on aluminum oxide is considered to represent only a beginning on the study of radiation effects in this material. A much more detailed study is necessary to determine the exact behavior of simple defects in this crystal structure, particularly as a function of temperature, before neutron transmission studies will be more fruitful. The outstanding factor which remains to be determined is the reason for the low fraction of defects retained at room temperature after irradiation. This, of course, speaks well for corundum as a stable structural material under the stress of high bombardment fluxes. A future experiment with the material irradiated and examined at low temperatures would be a profitable study and is contemplated as the equipment becomes available.

ACKNOWLEDGMENTS

The authors wish to express their appreciation to G. J. Dienes and G. H. Vineyard for their continued interest in this work and valuable contributions through discussions. They would like to thank P. W. Levy for his aid with the optical measurements attempted, and for his helpful comments concerning the data. They also wish to thank J. Sondericker and V. R. Field for their assistance with the experiment and reduction of data.

PHYSICAL REVIEW VOLUME 112, NUMBER 1 OCTOBER 1, 1958

Thermal Conductivity of Selenium at Low Temperatures

G. K. WHITE, S. B. WOODS, AND M. T. ELFORD*
Division of Pure Physics, National Research Council, Ottawa, Canada
(Received June 9, 1958)

Measurements are reported of the thermal conductivity of glassy selenium and polycrystalline metallic (hexagonal) selenium at temperatures from 2° to above 100°K. At the higher temperatures, the heat conductivity, λ, for the glassy solid is about 1 mw/cm deg. If we write $\lambda \approx \frac{1}{3}lCv$, then l, the mean free path, is of the order of the interatomic distance. On the other hand, for the high-purity metallic samples, $\lambda \cong 5/T$ w/cm deg. At low temperatures in metallic selenium, λ varies approximately as T^2, while in the glassy modification λ behaves in a similar fashion to that expected from earlier observations on soft glass and Pyrex.

INTRODUCTION

THE hexagonal form of selenium consists, like tellurium, of long spiral chains of atoms arranged in such a way that for each atom, in addition to the two nearest neighbors lying 2.316 A away in the same chain, four next-nearest neighbors lie in adjacent chains 3.467 A distant. This form has a density of 4.80 g cm^{-3} compared with about 4.30 g cm^{-3} for amorphous or glassy selenium. Some years ago one of us (GKW), at the suggestion of Dr. P. G. Klemens, measured[1] the heat conductivity below 100°K of a rod of glassy selenium (called Se 1) in order to see whether the dependence of its conductivity on temperature showed the same characteristic form found by Berman[2] for quartz glass, Phoenix glass, and Perspex and discussed in detail by Klemens.[3] This dependence is determined by the fact that at high temperatures, the disorder in the glass results in a phonon mean free path which is independent of the phonon frequency (and therefore of temperature), so that in the Debye expression for heat conductivity, $\lambda \simeq \frac{1}{3}Cvl$, where C is the specific heat per unit volume, v is the phonon velocity, and l, the mean free path for phonons, is of the order of the lattice

* National Research Council Postdoctorate Fellow.
[1] Performed at the Commonwealth Scientific and Industrial Research Organization, Division of Physics, National Standards Laboratory, Sydney, Australia.

[2] R. Berman, Proc. Roy. Soc. (London) **A208**, 90 (1951).
[3] P. G. Klemens, Proc. Roy. Soc. (London) **A208**, 108 (1951).

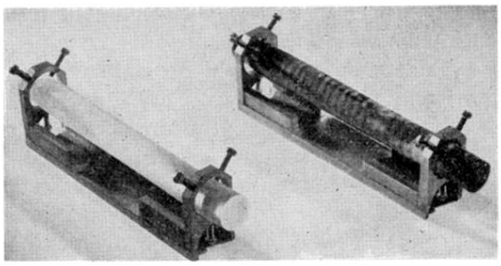

FIG. 1. Photograph of synthetic sapphire crystals used in these studies. The crystal at the left is unirradiated and that at the right has been irradiated to a total fast-neutron flux of $1.2\times10^{19}nvt$. The sample orientation is changed with the screws shown and the orientation is thereafter retained by the tray which accommodates the holders and interchanges their position in the beam. The crystals are approximately $\frac{5}{8}$ inch in diameter and 5 inches in length.